

Article

Two-Stage Integrated Optimization Design of Reversible Traction Power Supply System

Xiaodong Zhang ¹, Wei Liu ^{1,*}, Qian Xu ^{1,2} , Zhuoxin Yang ¹, Dingxin Xia ¹ and Haonan Liu ¹

¹ School of Electrical Engineering, Southwest Jiaotong University, Chengdu 610031, China; 2285694379@my.swjtu.edu.cn (X.Z.); xuqian@my.swjtu.edu.cn (Q.X.); isakia@my.swjtu.edu.cn (Z.Y.); xdx607287@my.swjtu.edu.cn (D.X.); liuhn@my.swjtu.edu.cn (H.L.)

² Department of Railway Engineering, Sichuan College of Architectural Technology, Deyang 618000, China

* Correspondence: liuwei_8208@swjtu.cn

Abstract: In a traction power supply system, the design of traction substations significantly influences both the system's operational stability and investment costs, while the energy management strategy of the flexible substations affects the overall operational expenses. This study proposes a novel two-stage system optimization design method that addresses both the configuration of the system and the control parameters of traction substations. The first stage of the optimization focuses on the system configuration, including the optimal location and capacity of traction substations. In the second stage, the control parameters of the traction substations, particularly the droop rate of reversible converters, are optimized to improve regenerative braking energy utilization by applying a fuzzy logic-based adjustment strategy. The optimization process aims to minimize the total annual system cost, incorporating traction network parameters, power supply equipment costs, and electricity expenses. The parallel cheetah algorithm is employed to solve this complex optimization problem. Simulation results for Metro Line 9 show that the proposed method reduces the total annual project costs by 5.8%, demonstrating its effectiveness in both energy efficiency and cost reduction.

Keywords: power supply; urban rail transit; adaptive management; optimal design



Academic Editor: Giovanni Lutzemberger

Received: 30 December 2024

Revised: 23 January 2025

Accepted: 31 January 2025

Published: 3 February 2025

Citation: Zhang, X.; Liu, W.; Xu, Q.; Yang, Z.; Xia, D.; Liu, H. Two-Stage Integrated Optimization Design of Reversible Traction Power Supply System. *Energies* **2025**, *18*, 703. <https://doi.org/10.3390/en18030703>

Copyright: © 2025 by the authors. Licensee MDPI, Basel, Switzerland. This article is an open access article distributed under the terms and conditions of the Creative Commons Attribution (CC BY) license (<https://creativecommons.org/licenses/by/4.0/>).

1. Introduction

Electrified rail transit has become a primary mode of urban transportation worldwide, with traction energy consumption accounting for about half of its total energy use [1]. Recently, many studies have focused on enhancing the operational efficiency of rail transit through improved utilization of regenerative braking energy [2,3]. However, the design of a traction power supply system, particularly the size and site of traction substations, plays an important role in ensuring the system's safe and stable operation. On the one hand, several studies have made relevant contributions to the design of systems. For instance, Xu [4] systematically optimized and designed the capacity configurations and locations of reversible substations using rectifier units and inverter feedback devices. However, it used fixed control parameters for system optimization design, whereas, in practice, the control parameters are not constant. Similarly, Ying [5] proposed a two-layer optimization method for the configurations of a flexible intelligent traction power supply system, achieving a remarkable 43.6% improvement in system efficiency. It does not account for special situations, such as the sudden power failure of a traction substation ("N-1" condition), which must be considered as it directly affects the operational safety of the system. Additionally, Huang [6] utilized energy storage devices to harness regenerative

braking energy, focusing primarily on the energy management of energy storage devices. However, few studies have achieved comprehensive optimization in regard to both energy management and the system design of reversible substations.

On the other hand, some studies focus on the energy management of traction power supply systems. For example, Ying [7] proposed a hierarchical energy management strategy that enhances the operational economy of flexible intelligent traction power supply systems while mitigating load fluctuations, but this study has limited consideration of real-time dynamic effects. Wang [8] employed model predictive control for the energy management of hybrid energy storage systems, enabling real-time optimization, but this method is relatively complex when applied to system optimization design due to the large power variations in trains, making predictions difficult. Chen [9] introduced an energy management approach that enhances power quality while reducing power consumption, but it does not regulate the traction substations.

To achieve real-time optimization and ensure more reliable and stable energy management, several studies have explored the application of fuzzy logic control. For instance, Ariche [10] implemented a fuzzy logic controller (FLC) for the energy management of electric vehicles equipped with energy storage. Experimental data demonstrated that fuzzy logic control significantly improves locomotive efficiency and adapts well to various operating conditions. Furthermore, Horrillo-Quintero [11] proposed a dynamic fuzzy logic energy management strategy for multi-energy microgrids which substantially reduced electrical energy consumption. Bai [12] established a fuzzy predictive control method for real-time train control, achieving a 4% reduction in train energy consumption. Wang [13] applies fuzzy logic control to flexible traction power supply systems, enabling adaptive control of the droop rate at traction substations with some energy-saving effects. However, the parameter selection for the fuzzy logic control in this method is somewhat arbitrary, and no in-depth study has been conducted on the selection of fuzzy logic control parameters.

In conclusion, some studies have focused on energy management systems, while others have concentrated on system design issues. These two aspects are closely interrelated, and the interaction between them has a significant impact on the overall system performance. In this paper, both energy management and system design are integrated into a comprehensive optimization problem. The optimization process is divided into two stages, addressing both aspects simultaneously. The main contributions of this paper are as follows.

- (1) A novel two-stage optimization method for flexible DC traction power supply systems is proposed which considers the optimization of both traction substation control parameters and system configuration. An adaptive droop rate control strategy based on fuzzy logic is applied in this design to enhance the utilization of regenerative braking energy.
- (2) To address the computational complexity of the optimization process, the parallel cheetah algorithm is introduced. By comparing various optimization algorithms, the results show that it not only significantly reduces computational time but also ensures faster convergence and more accurate results, offering a practical solution for real-world system design.
- (3) The proposed method is verified using the simulation of Metro Line 9, and the energy management effect under different headways is analyzed. The optimized design results of the traction power supply system are also analyzed.

2. Adaptive Control Strategy for Reversible Converter

2.1. The Traction Power Supply System with Energy Management

The simulation platform for the traction power supply system in urban rail transit comprises the main substation, a traction substation equipped with a reversible converter,

and the train, as depicted in Figure 1. Within this setup, the traction substation module incorporates a reversible converter (RC), which serves dual functions: providing power to the train and facilitating the return of regenerative braking energy to the medium-voltage network for efficient utilization [14]. Additionally, the traction station control module regulates the output voltage of the RC. It generates duty cycle signals to control the switching of Insulated Gate Bipolar Transistors (IGBTs) within the RC [15], based on an energy management strategy that integrates information from both the substation and the train.

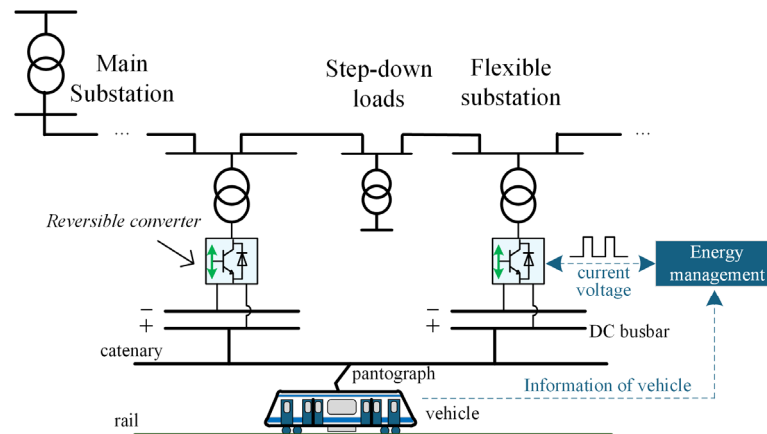


Figure 1. The DC traction power supply system.

2.2. The Control Method of Reversible Converter

Based on the external output characteristics of the reversible converter, the control strategy typically employs traditional voltage-current dual closed-loop control methods [15]. Referring to the droop characteristic of the reversible converter, by detecting the traction substation current I and multiplying it by the droop rate r , the command voltage U_{ref} is obtained. U_0 and U_1 are the work voltages of rectification and inversion. A comparison between the traction substation port voltage and the command voltage U_{ref} determines whether the traction substation operates in the rectifier state and the inverter state or enters a shutdown state. The current control command is derived through a PI controller, which regulates the output current of the traction plant to match the reference current value. In this paper, droop control is utilized, and its mathematical expression is provided as follows:

$$U_{ref} = \begin{cases} U_0 - r \cdot I, & I > 0 \\ U_1 - r \cdot I, & I < 0 \end{cases} \quad (1)$$

It should be noted that, when U_{ref} is within the range of U_0 and U_1 , the traction substation is subsequently switched off, causing the current to drop to zero.

2.3. Energy Management Strategy Based on FLC

The catenary voltage is regulated by a reversible converter. Variations in traction network voltage among different traction stations influence the overall energy flow within the system. When one train brakes while another is traction-powered, the output voltage can be adjusted to enable the regenerative braking energy to be absorbed by the neighboring train. If the braking energy exceeds a certain threshold, the regenerative energy can be used by medium-voltage (MV) loads. When the droop rate of the converter at the traction station is fixed, the dynamic interactions between trains are constantly changing. A large droop rate may hinder the timely inversion of regenerative braking energy back to the MV network, leading to energy wastage. Conversely, a small droop rate may prevent neighboring trains

from effectively utilizing the regenerative braking energy among themselves, resulting in energy waste.

In response to the complex nature of energy flow and the dynamic variations in train power, fuzzy logic control emerges as a superior approach for decision-making and control in complex and uncertain environments. An adaptive adjustment method for the droop rate of a reversible converter based on fuzzy logic control is introduced in this paper, aimed at achieving comprehensive energy management for the entire line. As illustrated in Figure 2, the proposed approach is primarily divided into two modules: the same-state control module and the different-state control module. Initially, the system determines whether the traction power exceeds 0 and calculates the sum of the train powers within a specified interval, assessing whether their signs (positive or negative) are consistent. Based on these two states, corresponding fuzzy control rules are designed. Subsequently, the absolute value of the traction power, the sum of the train powers within the interval, and the absolute value of the power difference between these powers serve as inputs, while the adjustment amount for the droop rate constitutes the output.

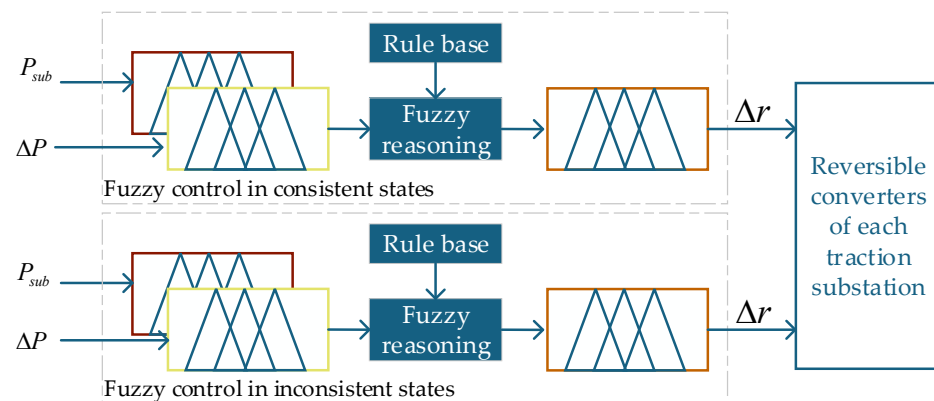


Figure 2. Energy management strategy based on FLC.

The inputs to the fuzzy control module consist of the absolute value of the substation power (P_{sub}) and the difference (ΔP) between the sum of the powers (P_{tr}) of the trains within the interval and the substation power; the output is the adjustment amount of the droop rate (Δr). The expression for ΔP is given by

$$\Delta P(t) = \left| \sum_n P_{tr}(t) - P_{sub} \right| \quad (2)$$

where $P_{sub} < 0$ means inverter mode, $P_{sub} > 0$ means rectifier mode, and t is the current time. The adjusted rectification and inversion droop rates are, respectively

$$r_{inv}(t) = r(t) - \Delta r \quad (3)$$

$$r_{rec}(t) = r(t) - \Delta r \quad (4)$$

In addition, the droop rate adjustment needs to satisfy the following constraint:

$$r_{\min} \leq r \leq r_{\max} \quad (5)$$

where r_{\min} is the minimum droop rate and r_{\max} is the maximum droop rate.

The fuzzy logic control rules are presented in Table 1. The logic terms “S, M, B” are small, medium, and big, respectively, while “NB, NS, O, PS, PB” signify negative big, negative small, zero, positive small, and positive big, respectively. When the signs (positive

or negative) of the traction power and the sum of the interval train powers are the same, the difference between these two powers ($\Delta P(t)$) is assessed. If the difference is small, the traction power (P_{sub}) is evaluated. If P_{sub} is small, the droop rate remains unchanged. If P_{sub} is moderate, the droop rate is slightly increased. If P_{sub} is large, the droop rate is increased more significantly. When the signs of the P_{sub} and the sum of the interval train powers differ, the difference between these two powers is again assessed. If the difference is small, in this condition, regardless of whether P_{sub} is small, moderate, or large, the droop rate is slightly increased. The remaining rules are detailed in Table 1.

Table 1. Rule of fuzzy control.

Is the Status Consistent?	Input1: $\Delta P(t)$	Input2: P_{sub}		
		S	M	B
Yes	S	O	PS	PB
	M	NS	O	PS
	B	NB	NS	O
No	S	PS	PS	PS
	M	PS	PS	PB
	B	PS	PB	PB

In this paper, triangular and trapezoidal shapes are employed for the membership functions (MFs) of both input and output variables. As illustrated in Figure 3, to simplify calculations, symmetric membership functions are utilized. Here, x_1 and x_2 represent the parameters of the MF for the input traction power P_{sub} , x_3 and x_4 denote the parameters of the MF for the input variable $\Delta P(t)$, and x_5, x_6, x_7, x_8, x_9 are the parameters of the MF for the output variable Δr . The inputs are fuzzified and then reasoned using fuzzy logic rules, and the outputs are de-fuzzified and finally sent to the controller of the converter to regulate the droop rate.

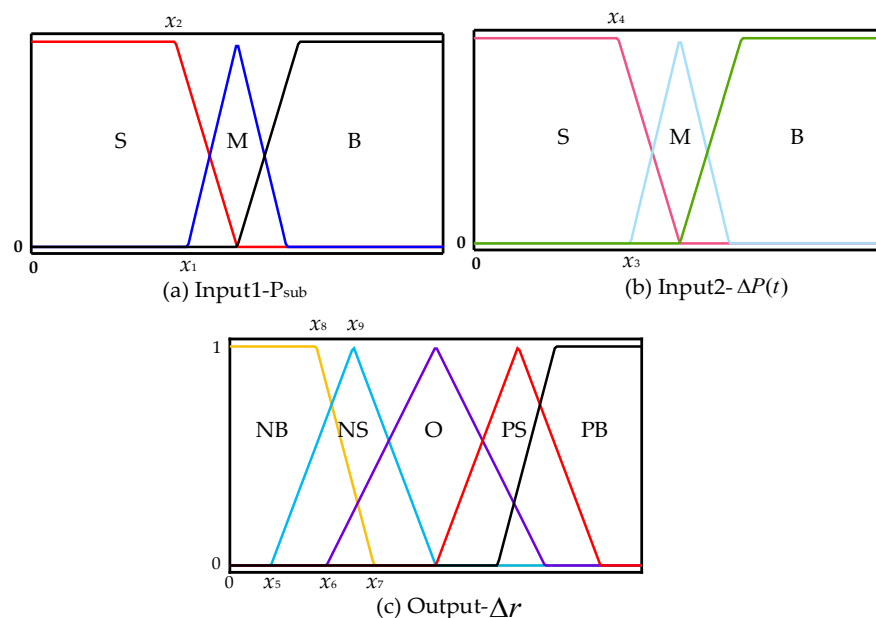


Figure 3. Membership functions of input and output variables.

3. Optimal Design of Traction Power Supply System

The optimization design of the traction power supply system encompasses the determination of traction substation locations, the capacity of reversible converters, and the specification of contact network parameters. Furthermore, recognizing the impact of energy

management strategies on economic efficiency and energy conservation, the parameters of the fuzzy membership function are adopted as optimization decision variables. This paper proposes a comprehensive optimization method for system design and energy management parameters. An objective function is formulated to minimize the overall cost of the traction power supply system, incorporating investment and maintenance costs, as well as traction energy consumption costs. Specifically, investment costs in traction substations consist of construction expenses for the traction station, costs associated with the capacity of the reversible converters, and construction costs for the catenary. Notably, the costs related to passenger stations, step-down stations, and rails are excluded from this analysis.

3.1. Objective Function

The objective function is presented in Equation (6).

$$\min F(X_1, X_2, X_3) = f_1(X_1, X_2) + f_2(X_1, X_2) + f_3(X_1, X_2, X_3) \quad (6)$$

This function incorporates three components: f_1 , representing the converted annual construction investment costs of the system; f_2 , denoting the converted annual equipment maintenance costs; and f_3 , signifying the converted annual operating cost of the power supply system. The decision variables include X_1 , which pertains to the location and capacity of the traction substation; X_2 , concerning the selection of the overhead contact system, encompassing the choice of contact rails, the catenary, the running rails, and the fourth rail; and X_3 , which relates to the parameters of the fuzzy membership functions employed within the energy management system. The expressions are shown in Equations (7)–(9), respectively.

$$X_1 = \begin{bmatrix} \sigma_1, \sigma_2, \dots, \sigma_i, \dots \\ C_1, C_2, \dots, C_i, \dots \end{bmatrix} \quad (7)$$

$$X_2 = [a, b] \quad (8)$$

$$X_3 = [x_1, x_2, \dots, x_9] \quad (9)$$

where σ_i is a binary random variable (0 or 1), indicating whether the i -th station is equipped with a traction substation, and where a value of 1 signifies that the station is equipped. The variable C_i represents the capacity of the reversible converter unit, measured in MW. Additionally, a and b denote the parameters associated with the contact network and the rails, respectively, while x_i represents the parameter of the fuzzy membership function.

3.1.1. Investment Cost

The total cost of the traction power system is outlined in Equation (10), which comprises several components. Specifically, the annual cost of the substation is detailed in Equation (11), the annual cost of the reversible converter is presented in Equation (12), and the annual cost of the catenary is specified in Equation (13).

$$f_1 = E_{sub} + E_{rc} + E_{sys} \quad (10)$$

$$E_{sub} = \sum_i^n \sigma_i B_{sub} \cdot \frac{d(1+d)^{y_{sub}}}{(1+d)^{y_{sub}} - 1} \quad (11)$$

$$E_{rc} = \left(\sum_i^n \sigma_i B_{rc} + \sum_i^n \sigma_i C_i M \right) \cdot \frac{d(1+d)^{y_{rc}}}{(1+d)^{y_{rc}} - 1} \quad (12)$$

$$E_{sys} = (B_{sysx1} + B_{sysx2}) \cdot \frac{d(1+d)^{y_{sys}}}{(1+d)^{y_{sys}} - 1} \quad (13)$$

where B_{sub} represents the construction cost of each traction substation. The variables y_{sub} , y_{rc} , and y_{sys} denote the desired service lives of the traction substation, reversible converter, and catenary system, respectively. The interest rate is denoted by d , and n signifies the total number of stations. Additionally, B_{rc} stands for the basic unit cost of the reversible converter, the unit is Chinese yuan per watt (CNY/W). Furthermore, B_{sysx1} and B_{sysx2} represent the construction costs of the catenary and the return track, respectively.

3.1.2. Maintenance Cost per Year

The maintenance cost of the traction power supply system mainly includes the maintenance of equipment, as the more equipment, the higher the maintenance cost. To simplify the calculation, the maintenance cost is estimated as the coefficient of the investment cost. Then, the annual maintenance cost formula is as follows:

$$f_2 = \alpha \times (E_{sub} + E_{rc} + E_{sys}) \quad (14)$$

where α is a coefficient between maintenance and construction costs, which typically ranges from 1 to 1.5 percent [16].

3.1.3. Energy Consumption Cost per Year

For energy management, fuzzy control is utilized, which aims to reduce the energy consumption of the power supply system. Additionally, the overall cost can be further lowered through the optimal design of the power supply system. Taking into account the potential impact of reverse power flow from urban rail transit back to the main substation on the power grid, this paper proposes incorporating the reverse power W_r as a penalty term to reduce reverse power flow. The calculation of the system's power supply energy consumption is presented in Equation (15).

$$f_2 = 365 \times \eta \times \sum_j (W_{tr} - W_f + \omega \cdot W_r) \times H_j \quad (15)$$

where W_{tr} represents the rectified energy of the traction substation, W_f is the feedback energy, and W_r denotes the energy returned back to the main substation, both measured in kW. η is the price of electricity, and the unit is kW/CNY. ω is used to limit the inverse power. H_j signifies the number of the j -th headway within a day.

3.2. Constraints

The design of the traction power supply system must prioritize ensuring the reliability of the power supply. Specifically, when one of the traction stations is shut down due to a fault, the catenary voltage of the power supply system must continue to meet the specified requirements. Consequently, constraints related to the catenary voltage, such as those outlined in Equation (16), are essential.

$$u_c^y \geq u_{cmin} \quad (16)$$

where u_c^y is the catenary voltage at any point along the entire line when any single traction substation is faulty. Specifically, u_{min} represents the minimum catenary voltage, which is set at 1000 V for a DC1500 V power supply system.

Concurrently, during normal operations, train functionality must meet the constraints of catenary voltage and rail potential, as outlined in Equations (17) and (18).

$$u_{cmin} \leq u_c \leq u_{cmax} \quad (17)$$

$$|u_r| \leq u_{r\max} \quad (18)$$

where u_c and u_r are catenary voltage and rail potential, respectively. The maximum catenary voltage $u_{c\max}$ is set at 1800 V. Additionally, the maximum value of the rail potential $u_{r\min}$ is set at 120 V.

3.3. Framework of the Optimal Design

The optimization parameters for the model presented in this paper encompass both system configuration parameters and control parameters within energy management. Consequently, a two-stage optimization framework is introduced to address this problem.

As illustrated in Figure 4, the first stage involves the utilization of an optimization algorithm to generate configuration solutions X_1 and X_2 for the traction power supply system. For each X_1 , the corresponding “N-1” operating scenarios are established, yielding solutions $X_1(1)$, $X_1(2)$, ..., $X_1(i)$, and so forth. For each $X_1(1)$, an analysis of power supply trends is conducted under rush hour headway. Simultaneously, the maximum droop rate is employed as the control parameter for the reversible converter. During the simulation, the catenary voltages are documented. Solutions that fail to meet the established constraints are discarded, while those that comply proceed to the second stage.

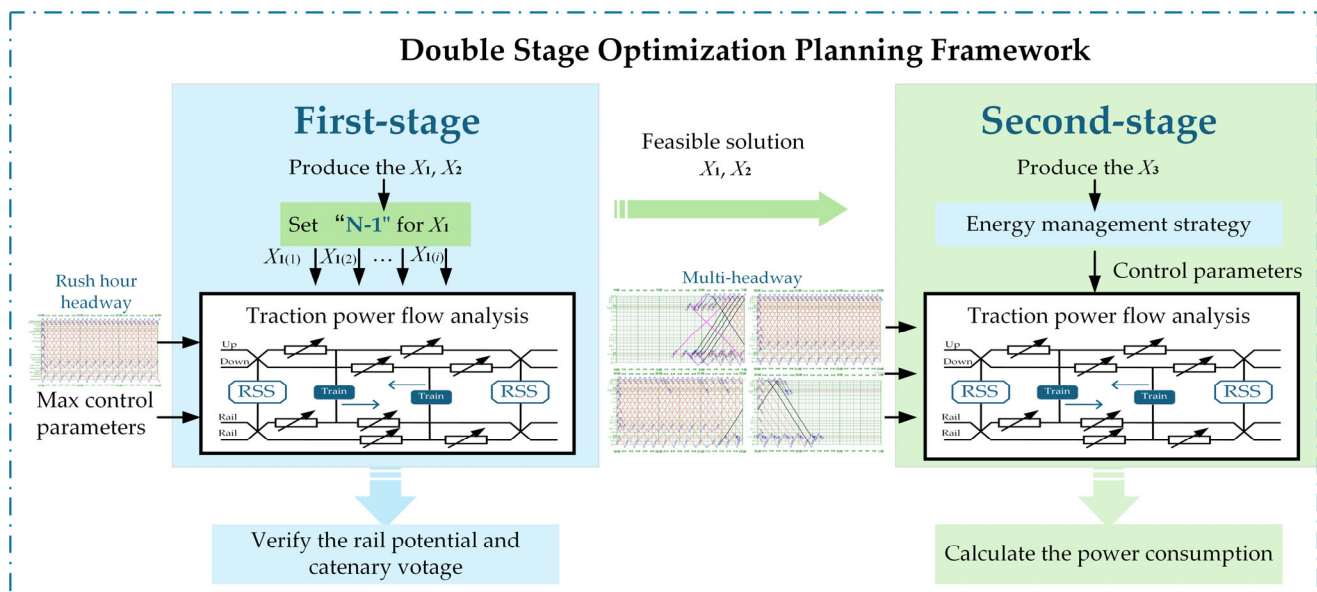


Figure 4. The framework of two-stage optimization planning.

In the second stage, the optimization algorithm determines the parameter X_3 of the fuzzy membership function. Subsequently, power flow simulations are conducted for various headways, incorporating the system configuration solutions X_1 and X_2 obtained from the first stage. These simulations yield the annual power consumption of the traction power supply system. Ultimately, the value of the objective function is computed.

3.4. Solution Process

The model introduced in this paper possesses a great number of optimization parameters and necessitates a long time for the “N-1” condition assessment in the first stage, leading to an extended model solution time.

To mitigate this issue, the paper integrates the parallel cheetah algorithm, as shown in Figure 5, for model resolution, leveraging the computer’s parallel thread pool by allocating multiple individuals from the population to the pool to expedite computation. The cheetah

algorithm [17] is adopted to solve the proposed model, with the steps being outlined as follows:

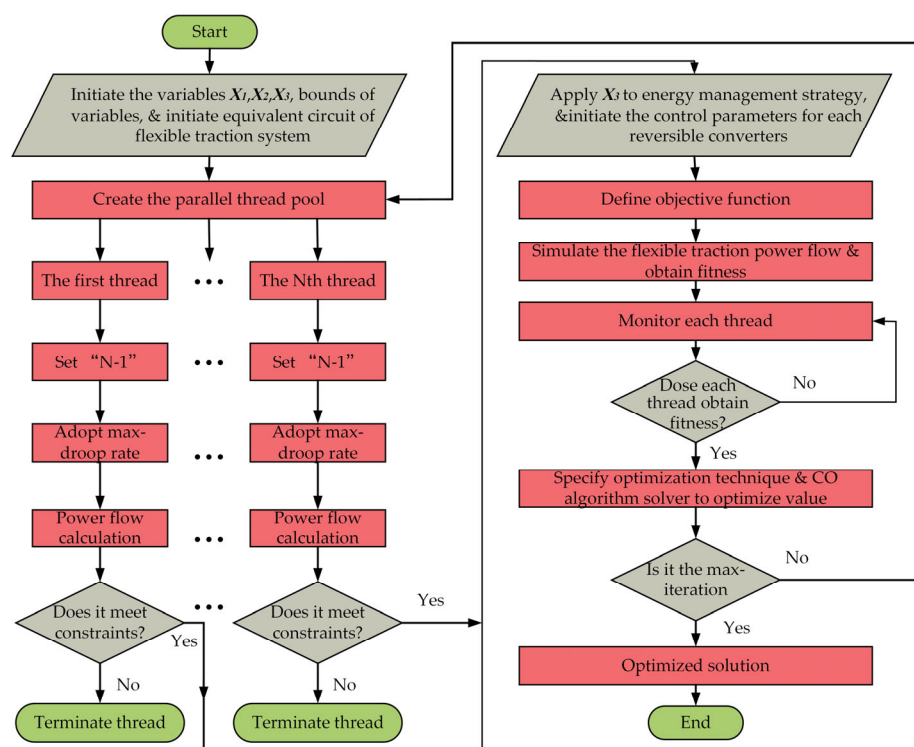


Figure 5. The solution flowchart of the proposed model.

Step 1: Set the population size, and maximum number of iterations for the algorithm, and establish the maximum number of threads for parallel computing.

Step 2: Randomly initialize the capacity and location of the traction substations, along with the parameters of the catenary, the parameters of the fuzzy logic control function, and the equivalent circuit of the power supply system.

Step 3: For each thread, based on the initial solution, configure “N-1” operating conditions. The reversible converter adopts the maximum droop rate and performs power flow simulation. If the constraints on catenary voltage are met, proceed to the next step; otherwise, terminate the thread.

Step 4: Incorporate the initialized parameters of the MF into the energy management strategy to derive the droop rate of the reversible converter for each traction substation.

Step 5: Define the objective function according to [6]. Conduct power flow calculations to obtain the fitness value for each thread. Monitor the status of each thread to determine if it has obtained a fitness value. If not, continue waiting for detection. Upon obtaining the fitness value, utilize the updated formula of the cheetah algorithm to identify the optimal solution. Then, determine if it is the maximum number of iterations. If not, return to the main thread to continue iterating. Upon reaching the maximum number of iterations, the optimal solution is obtained.

4. Case Study and Discussion

4.1. Simulation Conditions

Take Metro Line 9 as an example; the whole line is 15.849 km and includes 13 stations, as shown in Figure 6. In this paper, it is assumed that the sites of the traction houses are located within passenger stations. The passenger location information is detailed in Table 2; each station is equipped with a step-down station and the load ratio is set to 0.2. The capacity of the step-down station at the station is also given in Table 2.

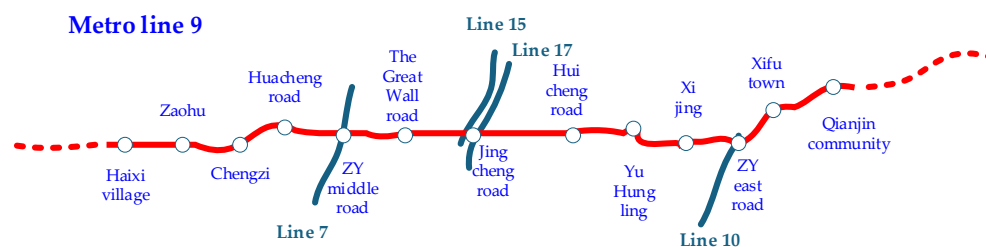


Figure 6. Route of Metro Line 9.

Table 2. Information of passenger station and step-down station.

Passenger Station	Position/km	Capacity/kVA
Haixi village	0	2 × 1250
Zaohu	1.890	2 × 1000
Chengzi	3.454	2 × 1000
Huacheng road	4.617	2 × 1000
ZY middle road	5.397	2 × 1000
Great Wall road	6.426	2 × 1250
Jingcheng road	7.486	2 × 1250
Huicheng road	9.334	2 × 1000
Yuhung road	10.689	2 × 1250
Xijing	11.866	2 × 1000
ZY east road	13.061	2 × 1250
Xifu town	14.288	2 × 1000
Qianjin Community	15.849	2 × 1250

The details of the power supply system used in the calculations for the case study are provided in Table 3. This includes the price and service life of various components of the traction power supply system, as well as the parameters of the main substation and the traction substations.

Table 3. Information on traction power supply system.

Item	Value
Running rail	resistance 0.02 Ω/km
Fourth rail	service life 30 years
	resistance 0.0083 Ω/km
	price 3.502 million CNY/km
Conductor rail	service life 30 years
	resistance 0.0083 Ω/km
	price 3.502 million CNY/km
Catenary	service life 30 years
	resistance 0.0173 Ω/km
	price 2.749 million CNY/km
Traction substation	service life 30 years
	price CNY 8 million
AC power supply	voltage level 110 kV
	main substation capacity 50 MVA
	short circuit capacity 1500 MVA
Industry electricity	price 0.78 CNY/kWh
Reversible converter	load losses 18.6 kW
	open circuit losses 3.4 kW
	Rectifier threshold voltage 1690 V
	Inversion threshold voltage 1700 V
	service life 20 years
	basic component cost CNY 0.2 million
	capacity related cost 400 CNY/kW

In this paper, the vehicle considered is a B-type car with six car formations (4M2T). Three kinds of headway are selected: 300 s, 257 s, and 134 s. The power and speed profiles for the individual trains during both the upward and downward travels are shown in Figure 7.

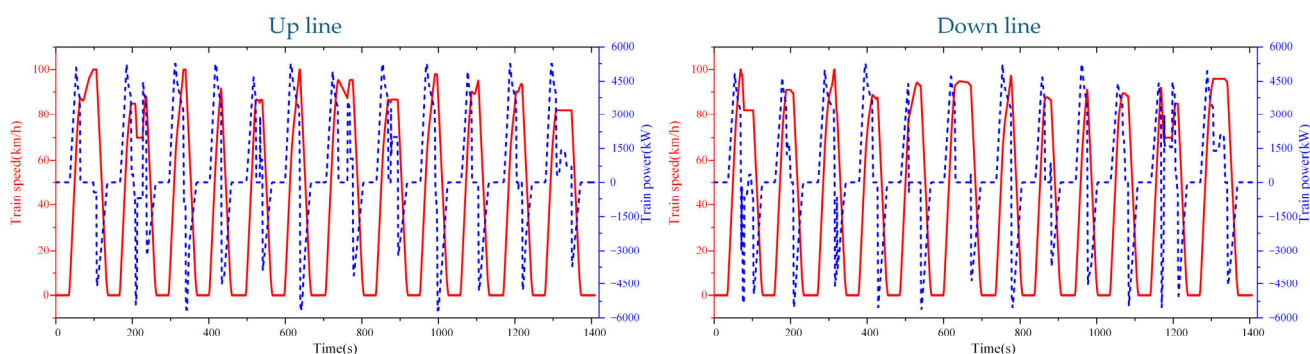


Figure 7. Train power and speed curves in the up-line and down-line.

4.2. Simulation Results

In this paper, the algorithm is executed on a workstation equipped with a 3.7 GHz processor and 64 GB of memory. Two cases are explored to analyze the system's performance. In Case 1, X_2 is designated as a fixed parameter, while X_1 and X_3 are identified as the optimization variables for system design. Alternatively, in Case 2, all three parameters (X_1 , X_2 , and X_3) are simultaneously considered as optimization variables.

For Case 2, a comparison is made among multiple heuristic parallel algorithms, namely the Particle Swarm Optimization (PSO), the Genetic Algorithm (GA), and the Cheetah Optimization (CO). For each algorithm, 50 individuals are set and 1000 iterations are carried out. It can be observed from Figure 8 that the parallel Cheetah Optimization algorithm achieves the best results. Therefore, it is employed for case simulation.

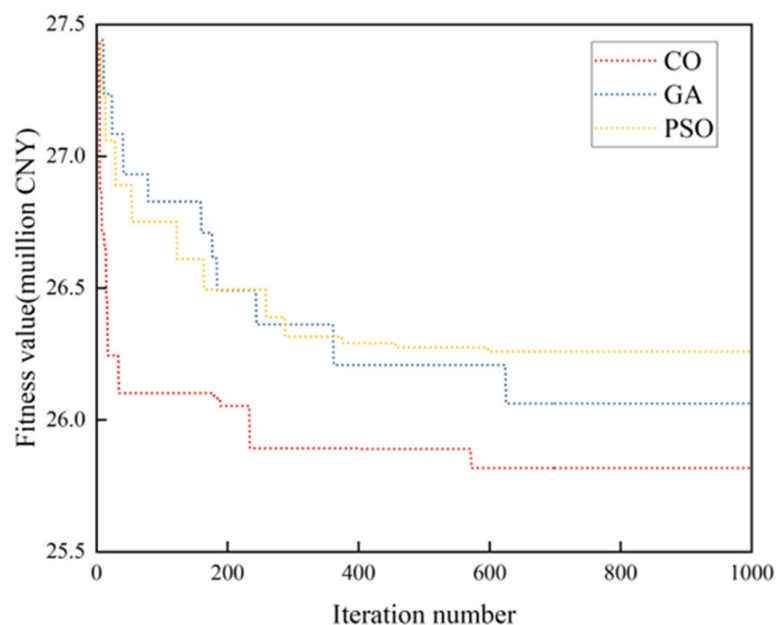


Figure 8. Convergence curve for different algorithms.

The iteration results for two cases in the traction power supply system are illustrated in Figure 9. The optimization result for Case 1 converges after 429 iterations, yielding an optimization objective value of CNY 26.37 million. In contrast, the optimization result for Case 2 converges after 571 iterations, achieving an optimization objective value of CNY

25.8175 million. When compared to Case 1, Case 2 demonstrates a reduction of 1.976% in the annual comprehensive economic cost.

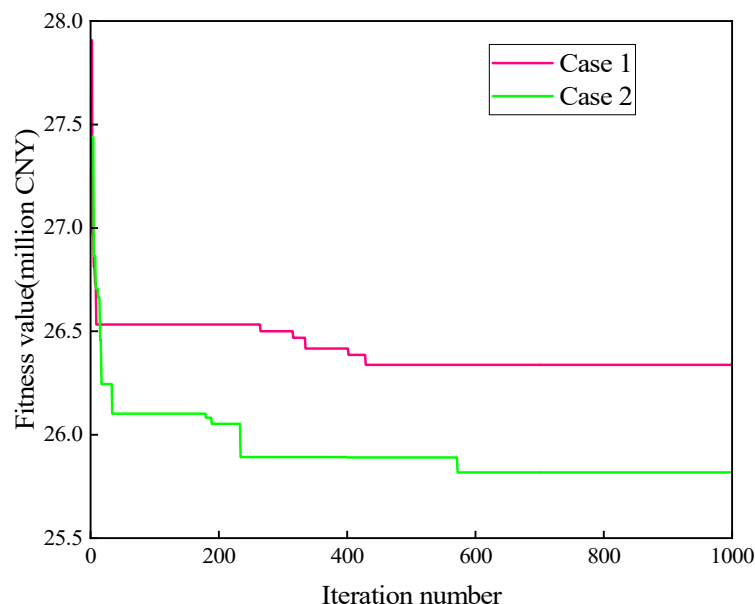


Figure 9. Convergence curve of different cases.

Comparing the results of Case 1 and Case 2, Table 4 presents the location and capacity of the traction substations for both optimized systems. Notably, both cases exhibit a total of six traction substations. The optimized system parameters selected include the catenary and steel rail configuration.

Table 4. Optimal configurations of Case 1 and Case 2.

Location of Traction Substations	Case 1	Case 2	Capacity/kVA	
			Case 1	Case 2
Haixi village	1	1	6500	6000
Zaohu	0	0	/	/
Chengzi	1	1	8000	8500
Huacheng road	0	0	/	/
ZY middle road	0	0	/	/
Great Wall road	1	1	6000	6500
Jingcheng road	1	0	6500	/
Huicheng road	0	1	/	6000
Yuhung road	0	0	/	/
Xijing	1	1	7000	8000
ZY east road	0	0	/	/
Xifu town	0	0	/	/
Qianjin Community	1	1	8000	7500

To verify the optimization results, the capacity configuration under Case 2 is set to the “N-1” condition to test the system safety performance at the rush hour headway (134 s), i.e., one of the traction substations is shut down, and the remaining five traction substations are utilized to supply power to the system to observe whether the voltage level meets the requirements. The catenary voltage in the “N-1” condition is shown in Figure 10, and it can be seen that the catenary voltage in every second is not lower than 1200 V, which meets the requirements of the power supply capacity.

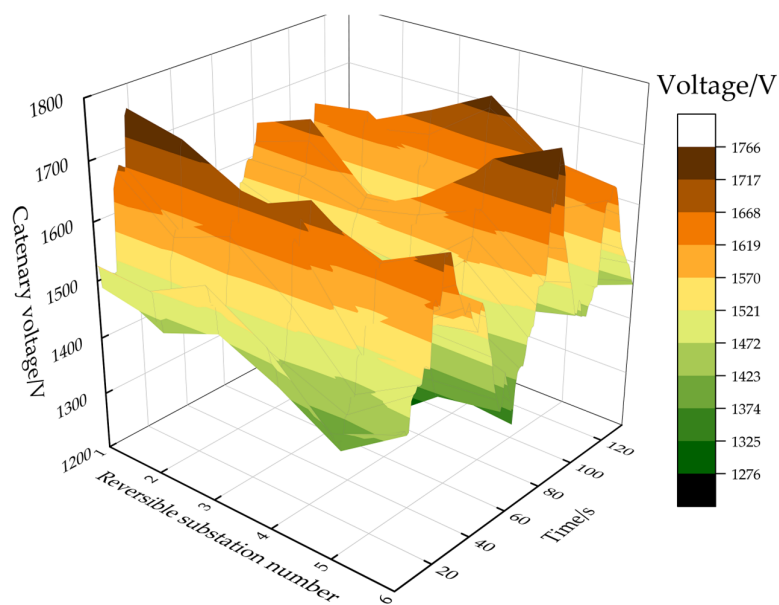


Figure 10. Catenary voltage under “N-1” condition.

4.3. Analysis of Energy Management Results

In Case 2, the fuzzy logic control parameters are optimized, with the results being presented in Table 5. These results indicate an improvement in the energy-saving rate of the traction power supply system when employing these optimized parameters for energy management.

Table 5. Parameters of the FLC.

Parameters of FLC	Optimal Value
x_1	3000
x_2	500
x_3	900
x_4	100
x_5	−4%
x_6	−2.5%
x_7	−1.5%
x_8	−3%
x_9	−2%

A comparison of operational energy consumption across three headways between Case 2 and Case 1 reveals the following: For a headway of 134 s, traction energy consumption decreases from 9315.68 kWh in Case 1 to 9098.536 kWh in Case 2, yielding a 2.33% energy saving. For a headway of 257 s, traction energy consumption is reduced from 4934.783 kWh in Case 1 to 4795.711 kWh in Case 2, representing a 2.81% energy saving. For a headway of 300 s, traction energy consumption drops from 4222.731 kWh in Case 1 to 4140.201 kWh in Case 2, resulting in a 1.95% energy saving, as shown in Figure 11.

To evaluate the effectiveness of the energy management method, energy consumption data for each headway are calculated. The traction power supply system provides power to the train, incorporating losses from catenary power transmission, medium-voltage AC cables, and the operation of the power supply equipment. As illustrated in Figure 12, the DC line loss of the catenary accounts for the largest percentage of total losses. Taking the 134 s as an example, Case 2 demonstrates a significant reduction in DC_loss from 865.701 kWh to 618.869 kWh, representing a 28.5% decrease compared to Case 1. For the equipment operating losses, namely DEV_loss and AC_loss, Case 2 exhibits a slight increase. This indicates that the primary focus of energy regulation is to minimize the line

transmission loss within the DC catenary. Consistent conclusions are observed for both the 257 s and 300 s.

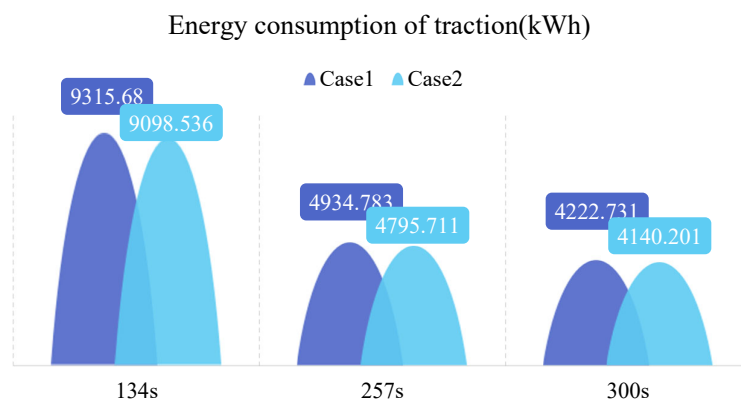


Figure 11. Energy consumption of the main substation in different cases and headway.

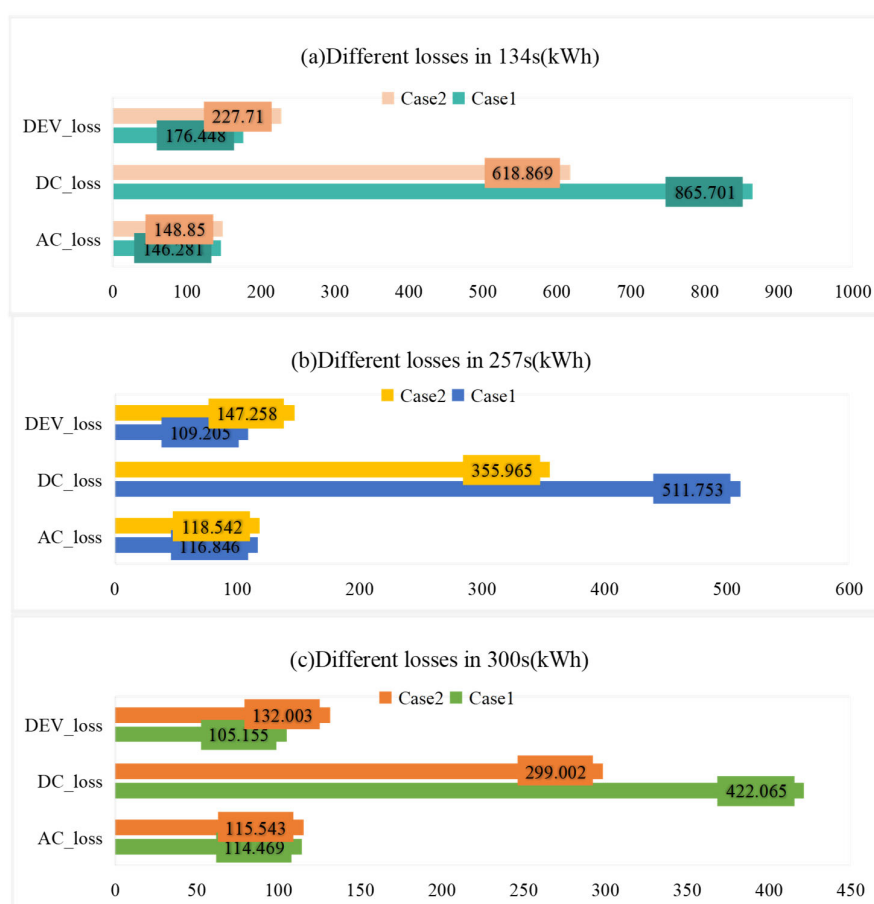


Figure 12. Different losses in different headways.

4.4. Economic Analysis of Different Cases

The total annual costs of the existing program are compared with those of Case 1 and Case 2.

As depicted in Figure 13. Case 1 and Case 2 exhibit 3.8% and 5.8% reductions in annual cost, respectively. These reductions are attributed to the decrease in the number of traction substations by two in both Case 1 and Case 2, leading to substantial savings in construction costs. As illustrated in Figure 14, Case 1 has the lowest annual construction cost, followed by Case 2. However, in terms of annual electricity cost, Case 1 is the highest and Case 2 is the lowest. Compared to the existing program, the annual electricity cost in

Case 2 is reduced by 1.53%, owing to optimized energy scheduling. Notably, the annual investment accounts for less than 22% of the total annual spend in each case, indicating that electricity costs constitute a larger portion of the annual costs. Therefore, the simultaneous optimization of energy scheduling management is particularly crucial.

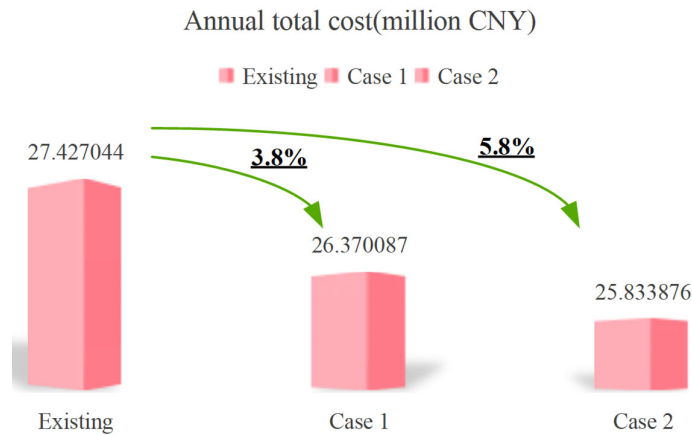


Figure 13. Comparison of annual total costs.

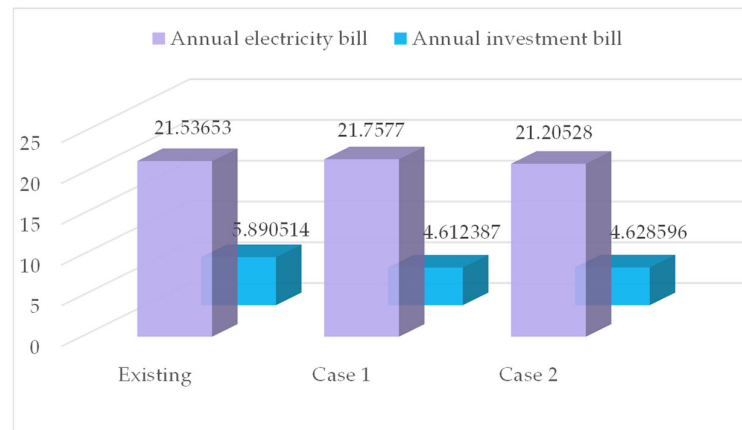


Figure 14. Comparison of annual electricity and investment costs.

5. Conclusions

In this paper, a two-stage optimal design for the traction power supply system is proposed, aiming to simultaneously optimize the capacity and location of traction substations, energy management parameters, and power supply system parameters. Using the actual Line 9 project as a case study, the optimal configuration of traction stations and energy management parameters for the entire line is determined. The optimization results indicate that, from the perspective of total annual cost, the selection of catenary and rail for power supply represents a superior solution. Through optimization, the number of traction stations is reduced from eight to six, while the capacity of each traction substation is increased from 4.0 MVA to 4.25 MVA. In terms of energy management, the primary energy savings stem from the reduction in line losses in the DC traction network. Compared to the existing program, the total annual cost is reduced by 5.8%, and the annual electricity cost is reduced by 1.53%, demonstrating the effectiveness of the proposed method. There are still some limitations in this study, and the optimization performance of fuzzy logic control in this system is generally not as effective as that of more advanced real-time control methods. In the future, we will focus on developing more effective real-time control strategies that can be better integrated with system design to achieve a more comprehensive system optimization.

Author Contributions: Conceptualization, X.Z., W.L. and Q.X.; methodology, X.Z., W.L. and Q.X.; software, X.Z., W.L. and D.X.; validation, X.Z., Q.X. and Z.Y.; formal analysis, X.Z.; investigation, X.Z.; resources, Q.X. and H.L.; data curation, X.Z., Q.X. and Z.Y.; writing—original draft preparation, X.Z., Q.X. and Z.Y.; writing—review and editing, X.Z., Q.X. and Z.Y.; visualization, X.Z., Q.X. and Z.Y.; supervision, W.L.; project administration, W.L.; funding acquisition, W.L. All authors have read and agreed to the published version of the manuscript.

Funding: This research was funded by the National Natural Science Foundation of China, grant number 52477125.

Data Availability Statement: Data are contained within the article.

Conflicts of Interest: The authors declare no conflicts of interest.

References

1. Hayashiya, H.; Iino, Y.; Takahashi, H.; Kawahara, K.; Yamanoi, T.; Sekiguchi, T.; Sakaguchi, H.; Sumiya, A.; Kon, S. Review of regenerative energy utilization in traction power supply system in Japan: Applications of energy storage systems in dc traction power supply system. In Proceedings of the IECON 2017—43rd Annual Conference of the IEEE Industrial Electronics Society, 29 October–1 November 2017; IEEE: Piscataway, NJ, USA, 2017. [\[CrossRef\]](#)
2. Ramsey, D.; Letrouve, T.; Bouscayrol, A.; Delarue, P. Comparison of Energy Recovery Solutions on a Suburban DC Railway System. *IEEE Trans. Transp. Electrification*. **2020**, *7*, 1849–1857. [\[CrossRef\]](#)
3. Hayashiya, H.; Akagi, M.; Konishi, T.; Okui, A. Survey of power electronics and electric machine application for on-site railway power system in Japan to realize eco-friendly transportation. In Proceedings of the 14th International Power Electronics and Motion Control Conference EPE-PEMC 2010, Ohrid, Macedonia, 6–8 September 2010; IEEE: Piscataway, NJ, USA, 2010. [\[CrossRef\]](#)
4. Xu, Q.; Liu, W.; Yang, Q.; Zhang, X.; Guan, H.; Deng, H.; Xiong, P. Bi-Level Optimal Design for DC Traction Power Supply System With Reversible Substations. *IEEE Trans. Transp. Electrification*. **2024**, *10*, 7488–7500. [\[CrossRef\]](#)
5. Ying, Y.; Tian, Z.; Wu, M.; Liu, Q.; Tricoli, P. Capacity Configuration Method of Flexible Smart Traction Power Supply System Based on Double-Layer Optimization. *IEEE Trans. Transp. Electrification*. **2023**, *9*, 4571–4582. [\[CrossRef\]](#)
6. Huang, Y.; Hu, H.; Ge, Y.; Liao, H.; Luo, J.; Gao, S.; He, Z. Joint Sizing Optimization Method of PVs, Hybrid Energy Storage Systems, and Power Flow Controllers for Flexible Traction Substations in Electric Railways. *IEEE Trans. Sustain. Energy* **2024**, *15*, 1210–1223. [\[CrossRef\]](#)
7. Ying, Y.; Liu, Q.; Wu, M.; Zhai, Y. The Flexible Smart Traction Power Supply System and Its Hierarchical Energy Management Strategy. *IEEE Access* **2021**, *9*, 64127–64141. [\[CrossRef\]](#)
8. Wang, Z.; Huang, Z.; Wu, Y.; Liu, W.; Li, H.; Peng, J. An Optimized Prediction Horizon Energy Management Method for Hybrid Energy Storage Systems of Electric Vehicles. *IEEE Trans. Intell. Transp. Syst.* **2024**, *25*, 4540–4551. [\[CrossRef\]](#)
9. Chen, J.; Ge, Y.; Wang, K.; Hu, H.; He, Z.; Tian, Z.; Li, Y. Integrated Regenerative Braking Energy Utilization System for Multi-Substations in Electrified Railways. *IEEE Trans. Ind. Electron.* **2023**, *70*, 298–310. [\[CrossRef\]](#)
10. Ariche, S.; Boulghasoul, Z.; Ouardi, A.E.; Bacha, A.E.; Tajer, A.; Espié, S. Dynamic Energy Optimization for Electric Vehicle Propulsion Using Fuzzy Logic. In Proceedings of the 2024 World Conference on Complex Systems (WCCS), Mohammedia, Morocco, 11–14 November 2024; pp. 1–6. [\[CrossRef\]](#)
11. Horrillo-Quintero, P.; García-Triviño, P.; Hoseinni, E.; García-Vázquez, C.A.; Sánchez-Sainz, H.; Ugalde-Loo, C.E.; Perić, V.S.; Fernández-Ramírez, L.M. Dynamic Fuzzy Logic Energy Management System for a Multi-Energy Microgrid. *IEEE Access* **2024**, *12*, 93221–93234. [\[CrossRef\]](#)
12. Bai, Y.; Ho, T.K.; Mao, B.; Ding, Y.; Chen, S. Energy-Efficient Locomotive Operation for Chinese Mainline Railways by Fuzzy Predictive Control. *IEEE Trans. Intell. Transp. Syst.* **2014**, *15*, 938–948. [\[CrossRef\]](#)
13. Wang, K.; Lin, F.; Yang, Z.; Wang, T.; Wei, X.; Fu, P. Fuzzy Logic Control Strategy of Substation Voltage in Urban Rail Flexible Traction Power Supply System. In Proceedings of the 2023 IEEE 3rd International Conference on Industrial Electronics for Sustainable Energy Systems (IESES), Shanghai, China, 26–28 July 2023; pp. 1–6. [\[CrossRef\]](#)
14. Xu, Q.; Liu, W.; Ding, J.; Tian, Z.; Zhang, J.; Zhang, X.; Bhatti, A.A. System-efficient Energy Regulation and Control for Reversible Substations in Urban Rail System. *IEEE Trans. Transp. Electrification*. **2024**, *in press*. [\[CrossRef\]](#)
15. Zhang, G.; Tian, Z.; Tricoli, P.; Hillmansen, S.; Wang, Y.; Liu, Z. Inverter Operating Characteristics Optimization for DC Traction Power Supply Systems. *IEEE Trans. Veh. Technol.* **2019**, *68*, 3400–3410. [\[CrossRef\]](#)

16. Xu, J. Research on Substation Locating and Sizing Based on Improved Firefly Algorithm. Master's Thesis, Department of Electrical Power Engineering, North China Electric Power University, Beijing, China, 2016.
17. Akbari, M.A.; Zare, M.; Azizipanah-Abarghooee, R.; Mirjalili, S.; Deriche, M. The cheetah optimizer: A nature-inspired metaheuristic algorithm for large-scale optimization problems. *Sci. Rep.* **2022**, *12*, 10953. [[CrossRef](#)] [[PubMed](#)]

Disclaimer/Publisher's Note: The statements, opinions and data contained in all publications are solely those of the individual author(s) and contributor(s) and not of MDPI and/or the editor(s). MDPI and/or the editor(s) disclaim responsibility for any injury to people or property resulting from any ideas, methods, instructions or products referred to in the content.